



HAL
open science

Levels and risk assessment of hydrocarbons and organochlorines in aerosols from a North African coastal city (Bizerte, Tunisia)

Badreddine Barhoumi, Javier Castro-Jiménez, Catherine Guigue, Madeleine Goutx, Richard Sempere, Abdelkader Derouiche, Amani Achour, Soufiane Touil, Mohamed Ridha Driss, Marc Tedetti

► To cite this version:

Badreddine Barhoumi, Javier Castro-Jiménez, Catherine Guigue, Madeleine Goutx, Richard Sempere, et al.. Levels and risk assessment of hydrocarbons and organochlorines in aerosols from a North African coastal city (Bizerte, Tunisia). *Environmental Pollution*, 2018, 240, pp.422 - 431. 10.1016/j.envpol.2018.04.109 . hal-01789427

HAL Id: hal-01789427

<https://amu.hal.science/hal-01789427>

Submitted on 12 May 2018

HAL is a multi-disciplinary open access archive for the deposit and dissemination of scientific research documents, whether they are published or not. The documents may come from teaching and research institutions in France or abroad, or from public or private research centers.

L'archive ouverte pluridisciplinaire **HAL**, est destinée au dépôt et à la diffusion de documents scientifiques de niveau recherche, publiés ou non, émanant des établissements d'enseignement et de recherche français ou étrangers, des laboratoires publics ou privés.

1 **Levels and risk assessment of hydrocarbons and organochlorines in aerosols from**
2 **a North African coastal city (Bizerte, Tunisia)**

3

4 Badreddine Barhoumi ^{a,b}, Javier Castro-Jiménez ^b, Catherine Guigue ^b, Madeleine Goutx ^b,
5 Richard Sempéré ^b, Abdelkader Derouiche ^a, Amani Achour ^a, Soufiane Touil ^a, Mohamed
6 Ridha Driss ^a, Marc Tedetti ^{b,*}

7

8 ^a Laboratory of Heteroatom Organic Chemistry, Department of Chemistry, Faculty of
9 Sciences of Bizerte, University of Carthage, 7021-Zarzouna, Tunisia

10 ^b Aix Marseille Univ., Université de Toulon, CNRS, IRD, MIO UM 110, 13288, Marseille,
11 France

12

13 *Corresponding author. Phone: +33 (0)4 86 09 05 27;

14 E-mail: marc.tedetti@mio.osupytheas.fr

15

16

17

18 Barhoumi, B., Castro-Jiménez, J., Guigue, C., Goutx, M., Sempéré, R., Derouiche, A.,
19 Achour, A., Touil, S., Driss, M.R., Tedetti, M., 2018. Levels and risk assessment of
20 hydrocarbons and organochlorines in aerosols from a north African coastal city (Bizerte,
21 Tunisia). *Environmental Pollution*, 240, 422-431.

22

23

24

25

26 **Abstract**

27 The aim of this study was to assess, for the first time, the concentrations, sources, dry
28 deposition and human health risks of polycyclic aromatic hydrocarbons (PAHs), aliphatic
29 hydrocarbons (AHs), polychlorinated biphenyls (PCBs) and organochlorine pesticides (OCPs)
30 in total suspended particle (TSP) samples collected in Bizerte city, Tunisia (North Africa),
31 during one year (March 2015 - January 2016). Concentrations of PAHs, AHs, PCBs and
32 OCPs ranged 0.5-17.8 ng m⁻³, 6.7-126.5 ng m⁻³, 0.3-11 pg m⁻³ and 0.2-3.6 pg m⁻³,
33 respectively, with higher levels of all contaminants measured in winter. A combined analysis
34 revealed AHs originating from both biogenic and petrogenic sources, while diesel vehicle
35 emissions were identified as dominant sources for PAHs. PCB potential sources included
36 electronic, iron, cement, lubricant factories located within or outside Bizerte city. The
37 dominant OCP congeners were *p,p'*-DDT and *p,p'*-DDE, reflecting a current or past use in
38 agriculture. Health risk assessment showed that the lifetime excess cancer risk from exposure
39 to airborne BaP was negligible in Bizerte, except in winter, where a potential risk to the local
40 population may occur.

41

42 **Keywords:** Atmospheric pollution; Total suspended particles; North Africa; Hydrocarbons;
43 Organochlorines

44

45 **Capsule:** Hydrocarbons and organochlorines in aerosols of Bizerte city (Tunisia) displayed
46 the highest concentrations, deposition fluxes and carcinogenic risks in winter.

47

48

49

50

51 **1. Introduction**

52 Airborne particles (aerosols), which are composed of hundreds of harmful constituents
53 ([Azimi et al., 2005](#)), have gained significant attention over past decades due to their impacts
54 on human health and ecosystems ([Dockery et al., 2000](#); [WHO, 2000](#)). Among these
55 constituents, hydrocarbons, including polycyclic aromatic (PAHs) and aliphatic hydrocarbons
56 (AHs), as well as organochlorines (OCs), including polychlorinated biphenyls (PCBs) and
57 organochlorine pesticides (OCPs), have attracted much interest due to their carcinogenic,
58 mutagenic and bioaccumulative effects, as well as their long-range atmospheric transport
59 (particularly OCs) ([Kim et al., 2013](#); [Wania and Mackay, 1996](#)).

60 PAHs are primarily emitted in the atmosphere by biomass and gas burning, incineration of
61 urban wastes, petrol and diesel combustion, as well as industrial processes ([Tobiszewski and](#)
62 [Namieśnik, 2012](#)), even though natural sources (volcanoes, forest fires) are not negligible
63 ([Mazquiarán and de Pinedo, 2007](#)). AHs are also emitted by anthropogenic activities (vehicle
64 emissions, coal, biomass and gas burning) but have significant biogenic sources, such as
65 higher plant waxes, pollen, and microbial activities ([Alves et al., 2012](#); [Perrone et al., 2014](#)).
66 PCB and OCP production and use were banned by the mid-1970s in most countries, but these
67 compounds remain present in all environmental media ([Haddaoui et al., 2016](#); [Pegoraro et al.,](#)
68 [2016](#); [Schröder et al., 2016](#)). Although the primary sources of PCBs are supposed to be
69 controlled ([Nizzetto et al., 2010](#)), i.e., transformers and capacitors, hydraulic fluids, additives
70 in paints and pesticides, plastics, landfills, and sludge drying beds ([Kim et al., 2013](#); [Lehmler](#)
71 [et al., 2010](#)), diffuse sources, such as accidental spills, combustion of different fuels, and re-
72 volatilization may have led to the current input of PCBs to the atmosphere ([Breivik et al.,](#)
73 [2002](#); [Dyke et al., 2003](#)). OCPs may enter the atmosphere during agricultural field
74 applications and in their evaporation from contaminated soils, water bodies and vegetation
75 ([Scholtz and Bidleman, 2006](#)).

76 PAH, AH, PCB and OCP concentrations have been largely reported in different
77 environments throughout the world (Stern et al., 1997; Valotto et al., 2017; Yao et al., 2002).
78 However, their measurements in aerosols of North African cities remain rare. In Tunisia, only
79 one preliminary study was conducted on PAHs associated with total suspended particles
80 (TSP) in Bizerte city (northern Tunisia) during the winter season (Ben Hassine et al., 2014).
81 In this context, the goal of the present study was to assess the levels, potential sources, dry
82 deposition and human health risks of PAHs, AHs, PCBs and OCPs in aerosols of Bizerte city.
83 Thereby, a one-year monitoring program was carried out for the collection of 60 aerosol
84 samples and the subsequent analysis of 94 organic compounds.

85

86

87 **2. Material and methods**

88

89 *2.1. Sampling site*

90

91 Sampling was conducted on the roof of the Faculty of Sciences of Bizerte (37° 16' 0.5802''
92 N, 9° 52' 49.875'' E; 8 m above ground level), approximately 1 km from the Bizerte city
93 center in Northern Tunisia, between the Mediterranean Sea and the Bizerte lagoon (Fig. S1 in
94 the supplementary information (SI)). Surrounding this site are heavily trafficked roads,
95 schools, residential areas and several industries, e.g., a petroleum refinery, cement
96 manufacturing, iron and steel metallurgy and bolt factory. Hence, the sampling site is well
97 representative of the Bizerte urban area (Castro-Jiménez et al., 2017). Bizerte is a medium-
98 sized city (~127,000 inhabitants), with economic activity focused mainly on agriculture,
99 fishing and operations of light and heavy industries, including cementery, plastic, textile,

100 mechanic and electronic manufacturing, iron and steel metallurgy, petroleum refining and
101 lubricants.

102 Generally, Bizerte has a humid climate, with an average temperature of 22°C, annual
103 precipitation rates varying between 300 and 800 mm, mainly concentrated in the fall and
104 winter months, and a hot summer and mild spring. The most frequent and strongest winds are
105 from the northwest (Ouakad, 2007).

106

107 **2.2. Aerosol sampling**

108

109 Aerosol samples were collected from March 2015 to January 2016 on precombusted
110 (450°C, 6 h) quartz fiber filters (QFFs) (Whatman QMA grade, 20.3 × 25.4 cm) using a high
111 volume air sampler (Tisch Environmental Inc., OH, USA) operating at an average flow of
112 0.66 m³ min⁻¹ for 48 h. Overall, 60 samples were collected along with five field blanks. Field
113 blanks were obtained by placing QFFs in the air sampler for a few seconds without switching
114 it on (Castro-Jiménez et al., 2016; Gioia et al., 2012). QFFs were then individually wrapped in
115 a double precombusted aluminum foil and stored in a freezer at -20°C before processing. The
116 pre- and post-sampling weights of the QFFs were determined using a microbalance after they
117 were placed in a desiccator (25°C) for 24 h. Each QFF was cut into two equal parts. One half
118 was used for pollutant analysis and the other half for the determination of TSP, organic
119 carbon (OC) and organic nitrogen (ON). Details regarding the sampling dates, meteorological
120 conditions and collected air volumes, as well as data on TSP, OC and ON concentrations for
121 each sample, are given in the SI (Table S1).

122

123 **2.3. Analysis**

124

125 Details on analytical procedures are presented in the [SI \(Text S1\)](#). Briefly, QFF filters were
126 cut into small pieces, spiked with a multi-standard mixture containing internal standards for
127 AHs (Hexadecane- d_{34} , tetracosane- d_{50} and hexatriacontane- d_{74}), PAHs (naphthalene- d_8 ,
128 fluorene- d_{10} , anthracene- d_{10} and pyrene- d_{12}), PCBs and OCPs (CB30, CB155 and CB198),
129 and extracted by Accelerated Solvent Extraction (ASE). The extracts were then purified using
130 silica-alumina columns and the analysis of native pollutants was subsequently performed
131 using gas chromatography coupled with a mass spectrometer (GC-MS) and an electron
132 capture detector (GC-ECD). The analyzed compounds included 34 PAHs (19 parents and 15
133 alkylated homologues), 28 AHs, 20 PCBs and 12 OCPs.

134 The concentrations of TSP in the QFFs were determined gravimetrically using the total and
135 impacted areas of the whole QFF, the area of the weighted QFF subsample, the mass of TSP
136 onto the QFF subsample, and the filtered air volume. OC and ON concentrations were
137 determined by high temperature combustion (CHN analyzer) ([Raimbault et al., 2008](#)).

138

139 ***2.4. Quality assurance and quality control (QA/QC)***

140

141 QA and QC included control/validation of laboratory and field blanks (procedures for
142 analysis and sampling, respectively), method recoveries (extraction, clean-up, analysis),
143 detection limits, analysis of certified reference material, and regular calibrations of the high
144 volume air sampler (each month), following the manufacturer's manual (Tisch
145 Environmental, HIGH VOL+). Blank samples were prepared, processed and analyzed in the
146 same manner as the field samples. Nap was detected in small amounts in the laboratory blanks
147 (< 5% of sample values), whereas CB-18, HCB and AHs (n -C₁₅– n -C₃₇) were detected in field
148 blanks (< 10% of sample values). Blank values for the individual compounds in aerosols are
149 presented in [Table S2](#). Average recoveries for AH, PAH and OC internal standards were 86,

150 84 and 91%, respectively. Instrument detection limits (IDLs) for all compounds were
151 determined as a signal-to-noise ratio (S/N) of 3 (Wolska, 2002). Method detection limits
152 (MDLs) were derived from the mean plus three times the standard deviation of the
153 concentrations in field blanks (considering an average sampled air volume of 960 m³). For
154 compounds that were not detected in field blanks, MDLs were based on their IDL. The MDLs
155 for hydrocarbons and OCs were in the range of 0.2-8 pg m⁻³ and 0.01-0.6 pg m⁻³, respectively
156 (Table S2). If the concentration of a given compound in a sample was below its MDL/IDL,
157 this compound was considered as not detected in the sample (below the limit of detection, <
158 lod).

159 The whole analytical procedure was validated by analyzing three replicates (0.1 g) of SRM
160 1649b (Urban Dust). A good agreement between the analyzed values and certified levels was
161 obtained for all compounds with recoveries varying from 82 to 104% (mean values) (Table
162 S3). All the data reported here were corrected for the blanks (laboratory and field blanks) but
163 not corrected for the recoveries.

164

165 *2.5. Statistical analysis*

166

167 Box-and-whisker plots, Pearson correlation matrix and principal component analysis
168 (PCA) were performed using XLSTAT 2013.5.01. No rotation technique was applied to PCA.
169 Non-parametric tests of Mann-Whitney (U-test) and Kruskal-Wallis (H-test), conducted with
170 Stat-View 5.0, were used to compare the distributions of two (U-test) or more than two (H-
171 test) groups.

172

173

174 **3. Results and discussion**

175

176 **3.1. Concentrations and molecular distributions**

177

178 **3.1.1. PAHs**

179 The concentrations of Σ_{34} PAHs in aerosols of Bizerte city over the study period displayed
180 a high variability, ranging from 0.5 to 17.8 ng m⁻³ (mean: 2.8 ± 3.4 ng m⁻³; median: 1.7 ng m⁻³)
181 ³) (Table S4), being in most cases < 5 ng m⁻³, while the highest value was recorded on 11
182 December (Fig. 1A). In the same area, Ben Hassine et al. (2014) recorded a Σ_{14} PAH
183 concentration of 25.4 ng m⁻³ in winter, which is higher than those measured in the present
184 study at the same season, very likely due a sampling site much more close to direct vehicular
185 traffic emissions. The measured concentrations in Bizerte were comparable with those
186 reported in Northwestern Mediterranean coastal cities (Chofre et al., 2016) and in the Western
187 and Southeastern Mediterranean Sea (Castro-Jiménez et al., 2012). However, they were lower
188 than those found in another north African coastal city, Algiers, Algeria (Yassaa et al., 2001),
189 in urban areas of the Eastern Mediterranean (Chrysikou and Samara, 2009; Ozcan and Aydin,
190 2009) and in Asian cities (Masih et al., 2010; Wu et al., 2014) (Table S5). Overall, PAH
191 concentrations found in Bizerte were lower than those recorded in other urban areas. This
192 could be explained by lower consumption of wood and fossil fuels for house heating and/or
193 less pronounced urban activities in Bizerte compared to the other sites.

194 The most abundant PAHs were BbF, BeP, IcdP and BghiP (Table S4; Fig. S2A). They
195 accounted for 38% of Σ_{34} PAHs (Fig. S3A). Logically, the annual ring distribution pattern
196 shows the dominance of high molecular weight PAHs (HMW-PAHs) (67.3–76.9%), followed
197 by medium molecular weight PAHs (MMW-PAHs) (17.7–27.3%), while low molecular
198 weight PAHs (LMW-PAHs), known to be preferentially present in the air gaseous phase
199 (Zheng et al., 2005), were a minority (7%) (Fig. S2B).

200 Σ_{34} PAH concentrations showed marked seasonal differences (H-test, $p < 0.05$), with
201 significantly higher values in winter (mean: $8.7 \pm 6.5 \text{ ng m}^{-3}$; median: 7.9 ng m^{-3}), and
202 significantly lower in summer (mean: $1.2 \pm 1.0 \text{ ng m}^{-3}$; median: 0.9 ng m^{-3}), compared to the
203 other three seasons (U-test, $p < 0.05$) (Fig. S4A). The lower concentrations in summer may be
204 due to higher temperatures and solar irradiance, which favor PAH evaporation and
205 photodegradation (Masiol et al., 2013). In contrast, during the winter, the increase in domestic
206 and vehicular emissions along with lower dispersion conditions and a decrease in
207 photochemical reactions may promote the accumulation of PAHs at the lower atmosphere
208 (Wan et al., 2006). Most of individual PAHs exhibited higher concentrations in winter and
209 lower in summer (Fig. S2A). As a result, LMW-PAHs presented the largest contribution in
210 summer (7.5%) and the smallest contribution in winter (3.6%), while the contributions of
211 MMW- (30.9%) and HMW-PAHs (65.4%) remain large in winter (Fig. S2B). This seasonal
212 ring distribution pattern has been already observed in other urban areas (Kishida et al., 2009;
213 Ramírez et al., 2011).

214

215 3.1.2. AHs

216 The concentrations of Σ_{28} AHs over the study period ranged from 6.7 to 126.5 ng m^{-3}
217 (mean: $30.2 \pm 21.1 \text{ ng m}^{-3}$; median: 25.1 ng m^{-3}) (Fig. 1B; Table S4). The highest
218 concentrations were recorded on 7 and 14 May (125.8 and 88.2 ng m^{-3}), while during the rest
219 of the year, they were mainly $< 55 \text{ ng m}^{-3}$, suggesting that the May peaks were caused by a
220 specific event (see below). These AH concentrations were within the range of those reported
221 in Prato, Italy (Cincinelli et al., 2003), Algiers (Yassaa et al., 2001) and Hong Kong, China
222 (Zheng et al., 2000), but significantly lower than those observed in northwestern and Eastern
223 Mediterranean coastal cities (Gogou et al., 1994; Karanasiou et al., 2007), and in Qingdao,
224 China (Guo et al., 2003) (Table S5).

225 The most abundant AHs were *n*-C₂₉, followed by *n*-C₂₇, *n*-C₃₁ and *n*-C₂₅ (Table S4; Fig.
226 S5). These four congeners accounted for 55% of the total AHs (Fig. S3B). The mean
227 concentration of HMW AHs (*n*-C₂₂–*n*-C₄₀) (28.9 ng m⁻³) was significantly higher (U-test, *p* <
228 0.05) than that of LMW AHs (*n*-C₁₅–*n*-C₂₁) (1.0 ng m⁻³), and concentrations of the HMW
229 AHs with an odd-number of carbon atoms were higher than those with an even-number of
230 carbon atoms (Figs. S3B and S5). This molecular distribution profile, characterized by the
231 dominance of *n*-C₂₅–*n*-C₃₁, no odd/even predominance in the range of *n*-C₁₅–*n*-C₂₁ and odd
232 carbon number predominance in the range *n*-C₂₂–*n*-C₄₀ (Fig. S3B), was similar to that found
233 in the urban areas of Nanjing, China (Wang et al., 2006) and Rio de Janeiro, Brazil (Maioli et
234 al., 2009) and was indicative of mixed petrogenic and biogenic sources (Rogge et al., 1993a,
235 1993b, 1996).

236 The AH concentrations in spring (mean: 36.4 ± 30.0 ng m⁻³; median: 25.1 ng m⁻³), summer
237 (mean: 24.0 ± 13.6 ng m⁻³; median: 19.8 ng m⁻³), autumn (mean: 24.4 ± 12.8 ng m⁻³; median:
238 22.5 ng m⁻³) and winter (mean: 38.6 ± 18.5 ng m⁻³; median: 38.3 ng m⁻³) were not
239 significantly different from each others (H-test, U-test, *p* > 0.05) (Fig. S4B). The
240 concentrations of individual AHs in the ranges *n*-C₁₅–*n*-C₂₆ and *n*-C₃₃–*n*-C₄₀ were rather
241 higher in winter and spring, and lower in summer and autumn (Fig. S5). *n*-C₂₇, *n*-C₂₉ and *n*-
242 C₃₁ concentrations displayed a strong increase in winter, summer/spring and spring,
243 respectively. The higher levels of the biogenic *n*-C₂₉ and *n*-C₃₁ during spring and summer
244 could be due to the higher contribution of terrestrial vegetation through the mechanical
245 abrasion of higher plants, leaf waxes, vegetation debris, and soil erosion, while the highest
246 concentration of the biogenic *n*-C₂₇ in winter remains quite peculiar (Rogge et al., 1993b;
247 Górka et al., 2014).

248

249 3.1.3. PCBs and OCPs

250 The concentration of \sum_{20} PCBs averaged 3.5 ± 2.4 pg m⁻³ with a median value of 3.6 pg m⁻³
251 (Fig. 1C; Table S6). The highest \sum_{20} PCB concentration was found on 11 June (11.0 pg m⁻³),
252 and the lowest (0.3 pg m⁻³) on 10 July. Total PCB concentrations measured were within the
253 range of those reported for other Mediterranean coastal sites (Castro-Jiménez et al., 2011;
254 2017; Mandalakis et al., 2005) and some European inland areas (Castro-Jiménez et al., 2009;
255 Landlová et al., 2014), but they were lower than those recorded over the Mediterranean and
256 Black Seas (Berrojalbiz et al., 2014) and in highly urbanized Mediterranean and Asian areas
257 (Gregoris et al., 2014; Mandalakis et al., 2002; Ozcan and Aydin, 2009; Yeo et al., 2004)
258 (Table S5).

259 The most abundant PCB congeners were CB-180, -138 and -153 (Table S6; Fig. S6A),
260 accounting for 48% of \sum_{20} PCBs (Fig. S3C). Hence, the dominant PCB groups were Hexa-
261 CBs, Hepta-CBs and Penta-CBs (Table S6; Fig. S6B). This pattern of homolog profiles had
262 already been observed in Kyonggi-do, South Korea (Yeo et al., 2004).

263 Among the 12 analyzed OCPs, only 6 pesticides were detected in Bizerte aerosols (HCB,
264 γ -HCH, δ -HCH, Hepchl, *p,p'*-DDE and *p,p'*-DDT). The \sum_6 OCP concentrations ranged from
265 0.2 to 3.6 pg m⁻³ (mean: 1.1 ± 0.84 pg m⁻³; median: 0.76 pg m⁻³) (Table S6). The highest
266 concentrations were observed on 18 March and 23 December (Fig. 1D). Interestingly, March
267 and December are land laboring and cereal treatment periods, respectively, potentially
268 favoring soil-atmosphere pesticide transfer. \sum_6 OCP concentrations determined in Bizerte
269 were generally lower than those observed in other urban areas (Table S5). The most abundant
270 compounds were DDTs, including *p,p'*-DDT and *p,p'*-DDE, and Hepchl, accounting for 69
271 and 10% of \sum OCPs, respectively (Fig. S3D).

272 The highest \sum_{20} PCB and \sum_6 OCP concentrations were measured in winter (mean: 5.0 ± 2.6
273 pg m⁻³, median: 5.0 pg m⁻³ for PCBs; mean 2.1 ± 1.0 pg m⁻³, median: 2.2 pg m⁻³ for OCPs)
274 and the lowest in autumn for PCBs (mean 3.1 ± 1.4 pg m⁻³, median: 2.7 pg m⁻³) and in

275 summer for OCPs (mean $0.7 \pm 0.4 \text{ pg m}^{-3}$, median: 0.6 pg m^{-3}) (Fig. S4C and D).
276 Nevertheless, whereas no significant seasonal difference was found for $\sum_{20}\text{PCB}$
277 concentrations (H-test, U-test, $p > 0.05$) (Fig. S4C), $\sum_6\text{OCP}$ concentrations were significantly
278 higher in winter compared to the other three seasons (H-test, U-test, $p < 0.05$) (Fig. S4D).
279 Most individual PCBs and OCPs also exhibited higher concentrations in winter (Fig. S6A and
280 S7).

281

282 ***3.2. Influence of air mass origin and meteorological parameters***

283

284 Wind sector and backward trajectory analyses were carried out to assess the local and long-
285 range atmospheric transport of pollutants, respectively (Fig. 2). The dominant wind directions
286 were from the west-north-west (WNW) in spring, the WNW and the north-west (NW) in
287 summer and autumn, and the south-east (SE) in winter. This suggests that local emissions
288 from downtown Bizerte (vehicular exhaust), Bizerte harbor and the cement factory, located
289 NW of the site, and from Zarzouna area (petroleum refinery, the Tunisian Company of
290 Lubricants (SOTULUB)) and Menzel Jemil city (electronic, plastic, and textile industries),
291 located SE of the site, are the most likely to influence the pollutant levels observed in aerosols
292 (Fig. S1). In all cases, the highest concentrations occurred in winter when winds were from
293 the SE.

294 Back-trajectories were calculated using the NOAA Hysplit Model (Draxler and Rolph,
295 2011). As shown in Fig. 2, most of the air masses which reached the sampling site were of
296 oceanic origin with limited passage through the European continent. Although there is a
297 combined effect of remote air masses and local winds, the contribution of local sources and
298 neighboring cities to the contamination observed here is likely more important. Actually, in
299 addition to the apparent clean nature of the oceanic air masses, high wind speeds above the
300 Mediterranean Sea can disperse pollutants before they reach the sampling site. Indeed, we

301 observe a significant inverse relationship between wind speed (WS) and PAH/OCP
302 concentrations (Table S7). This suggests the predominance of local sources, as strong winds
303 flush pollutants out of the study area whereas weak winds allow pollutants to accumulate over
304 time (Hong et al., 2007).

305 Besides wind, it has been recognized that TSP amount, ambient temperature (AT) and
306 relative humidity (RH), may strongly affect pollutant concentrations in aerosols (Park et al.,
307 2002). In this region, AT was higher in summer/autumn and lower in spring/winter, while RH
308 showed little variation among the seasons. TSP concentrations ranged from 9.6 to 119.1 $\mu\text{g m}^{-3}$
309 ³ (mean: 62.0 $\mu\text{g m}^{-3}$) (Table S1). A significant positive correlation was observed between
310 PAH/OCP concentrations and RH (Table S7), suggesting that the latter can play an important
311 role in pollutant condensation on particulate matter. Mastral et al. (2003) showed that RH
312 influenced the PAH concentrations in aerosols possibly through its impact on PAH gas-
313 particle partitioning. Significant negative correlations were found between PAH/OCP
314 concentrations and AT (Table S7), indicating a possible temperature dependence on
315 atmospheric pollutants. Low temperatures may indeed stimulate the transfer of pollutants
316 from the gaseous to particulate phase, and inversely (Masiol et al., 2013). This observation is
317 in accordance with the aforementioned results, that is the highest and the lowest PAH/OCP
318 concentrations were recorded in winter and summer, respectively (Fig. S4).

319 PCA was carried out to obtain a picture of the relationships between all the measured
320 parameters (Fig. 3). Samples collected in winter had the highest Factor 1 scores, indicating
321 that PAHs, PCBs and OCPs were the dominant compounds in winter and were associated
322 with RH, OC and ON (Table S7). Samples collected in summer displayed the highest Factor 2
323 scores, suggesting that AT and WS were probably important parameters driving the low levels
324 of PAHs, PCBs and OCPs during the warm season. Some samples collected in spring were

325 loading on Factor 3, suggesting that AHs were important in spring due to biogenic activities,
326 as previously described.

327

328 **3.3. Potential sources**

329

330 **3.3.1. PAHs**

331 Molecular diagnostic ratios used to investigate PAH emission sources are reported in [Table](#)
332 [1](#). These ratios have to be taken with caution for the evaluation of PAH sources since they
333 may be modified with degradation and weathering of PAHs occurring from the source point
334 to the collection site ([Tobiszewski and Namiesnik, 2012](#)). The cross plots of BaA/(BaA +
335 Chr) (0.06-0.40) and IcdP/(IcdP + BghiP) (0.23-0.52) ratios and of Ant/(Ant + Phe) (0.00 to
336 0.31) and Flu/(Flu + Pyr) (0.25-0.67) ratios (Table 1 for values but cross plots not shown)
337 revealed a mixed source of PAHs (petrogenic and pyrogenic), with a strong contribution of
338 liquid fossil fuel combustion ([Mai et al., 2003](#); [Yunker et al., 2002](#)), as well as a small
339 contribution of biomass combustion ([Ravindra et al., 2008](#); [Tang et al., 2005](#)). Albeit no
340 industry using coal as fuel source (or coal burning for house heating) is present in the study
341 area, open burning of biomass is a common procedure in Bizerte for crop and forest residue
342 disposal and for land preparation.

343 The ratio of combustion PAHs (CPAHs, i.e., the sum of Flu, Pyr, BaA, Chr, BbF, BkF,
344 BaP, IcdP, BghiP) over $\Sigma 16$ US EPA PAHs (CPAHs/ $\Sigma 16$ US EPA PAHs) was ~ 1 , while the
345 BbF/BkF ratio was > 0.5 for all samples (Table 1). Their cross plot (not shown) suggested the
346 dominant contribution of diesel combustion. In addition, our BbF/BkF ratios, all higher than
347 0.5 (1.74–12.43), our IcdP/(IcdP + BghiP) ratios, mostly between 0.35 and 0.70, as well as
348 some Flu/(Flu + Pyr) ratios higher than 0.5 indicate diesel emissions ([Mai et al., 2003](#); [Manoli](#)
349 [et al., 2004](#); [Mirante et al., 2013](#); [Ravindra et al., 2008](#)). Indeed, extensive vehicular emissions

350 of heavy and light cars have been observed coming from the highway at 400 m from the
351 sampling site. Overall, these diagnostic ratios underline that PAHs in Bizerte aerosols are
352 mainly originating from vehicular traffic emissions and diesel combustion.

353

354 3.3.2. AHs

355 The calculated CPI, %Wax, UCM and Pr/Phy values are listed in [Table 1](#). CPI computed
356 as the ratio of odd to even numbered homologues, is an indicator of anthropogenic (CPI ~ 1)
357 or biogenic AHs (CPI higher than 3) ([Gong et al., 2011](#)). [Table 1](#) shows values for CPI₁
358 (whole range, *n*-C₁₅–*n*-C₄₀), CPI₂ (petrogenic AHs, *n*-C₁₅–*n*-C₂₅), and CPI₃ (biogenic AHs, *n*-
359 C₂₅–*n*-C₃₆) for the entire study period and four seasons. CPI₁ annually ranged 1.1–6.1, which
360 was very close to the range determined in Guangzhou, China ([Choi et al., 2016](#)) but higher
361 than that found in Rouiba (Algiers) and Wroclaw (Poland) ([Górka et al., 2014](#); [Moussaoui et](#)
362 [al., 2013](#)), likely because of a larger input from biogenic sources in Bizerte. CPI₁ was closer
363 to 3 in spring and summer than in autumn and winter, suggesting a higher contribution of
364 biogenic sources during the warmer seasons. CPI₂ ranged 0.96–8.4 over the study period
365 ([Table 1](#)), and the fact that almost all values were between 1 and 2 revealed a petrogenic
366 fingerprint. CPI₃ (1.2–8.8) displayed, as for CPI₁, higher values (higher than 3) in spring and
367 summer ([Table 1](#)), underscoring the influence of biogenic emissions from season-to-season.
368 CPI₂ and CPI₃ values determined in Bizerte are similar to those observed in Lhasa, China
369 ([Gong et al., 2011](#)) but higher than those in Nanjing, China ([Wang et al., 2006](#)). The plant
370 wax contribution to the total mass of the measured AHs (%Wax) in Bizerte aerosols was on
371 average 39.9, 45.0, 22.9 and 23.4% in spring, summer, autumn and winter, respectively
372 ([Table 1](#)). This indicated a higher input from leaf epicuticular waxes within the AH pool
373 during the warmer seasons. A highly significant positive correlation was found between
374 %Wax and CPI₁ at the annual level ($r = 0.93$, $p < 0.05$) showing that these two indices were

375 relevant in the source assignment of AHs (He et al., 2010). The stronger contributions of
376 biogenic sources in spring and summer may be due to growth of leaves, photosynthesis,
377 blooming, fungi and pollen spreading (Choi et al., 2016). Indeed, the study site is surrounded
378 by a varied vegetation cover, and mountains rich with deciduous and coniferous trees, which
379 may represent the main biogenic sources.

380 Unresolved complex mixture (UCM) has been identified in all samples (22.5–262.5 ng m⁻³)
381 (Table 1), denoting the presence of vehicular residues (Rogge et al., 1993a, b). It exhibits
382 higher concentrations in winter and spring, suggesting more fossil fuel utilization during the
383 cold seasons. Additionally, the presence of UCM together with isoprenoids Pr and Phy
384 confirms petroleum residue contamination (Andreou et al., 2008). However, in summer, the
385 highest Pr/Phy ratio (> 1.5), along with the lowest UCM values, may reflect the more
386 important contribution of biogenic sources.

387

388 3.3.3. PCBs

389 PCBs have been widely used in Tunisia since the 1970s, and despite an import ban in 1986
390 of any equipment containing PCBs, they can still be detected in Bizerte aerosols. Several
391 authors reported that the PCB pattern was directly related to meteorological conditions and air
392 mass transport (Diesch et al., 2012; Piazza et al., 2013; Yeo et al., 2003). Wania and Mackay
393 (1996) assumed that the heaviest homologues could easily be deposited on plants, soils and
394 surface waters, while the lightest ones, more volatile, were mostly present in the gaseous
395 phase and strongly affected by long-range atmospheric transport. The distribution of Penta-,
396 Hexa-, Hepta- and Tri-CBs in the Bizerte aerosols (Fig. S6B, Table S6) could be the result of
397 both short and long-range atmospheric transport. The high concentrations of the heaviest
398 homologues (Hexa- and Hepta-CBs) might be influenced by industrial emissions (the cement
399 factory) and intense shipping activities (Bizerte harbor), both very close to the sampling site

400 (to the NW). Previous studies have recorded PCBs in sediment and fish in the same area
401 ([Barhoumi et al., 2014a, b](#)). The presence of tetrachloro- (CB66), pentachloro- (CB101,
402 CB118, CB126), hexachloro- (CB128, CB138, CB153) and heptachloro-congeners (CB180)
403 in our samples is consistent with a contribution of commercial PCB mixtures Aroclor 1248,
404 1254 and 1260/1262 ([Takasuga et al., 2006](#)), which have been widely used in transformers
405 and electrical equipment in several countries ([Gregoris et al., 2014](#)). A large number of
406 transformers are still used or presently stored in unsatisfactory conditions, promoting their
407 atmospheric dispersion. In 2004, a study identified 1,079 PCB-contaminated transformers in
408 Tunisia, representing 720 tons of liquid PCBs ([APEK, 2005](#)). In view of industrial activities
409 around the sampling site (to the NW, SE and SW), it is assumed that the plastic, tire,
410 mechanic and electronic factories in Menzel Jemil city, the iron factory in Menzel Bourguiba
411 city (to the SW), the Bizerte cement factory, SOTULUB in Zarzouna area, the incineration of
412 contaminated equipment, and the combustion of different fuels were significant sources of
413 PCBs in Bizerte aerosols.

414

415 **3.3.4. OCPs**

416 As previously discussed, HCB, *p,p'*-DDT and *p,p'*-DDE showed the highest frequency of
417 detection in aerosols, despite their ban since 1984 ([APEK, 2005](#)). HCB occurrence may be
418 ascribed not only to its past use as a fungicide treatment for seeds, but also to the fact that it
419 can be released from certain thermal processes in the metallurgical industry and at oil
420 refineries, and from waste incineration and motor vehicles. It may also be present as impurity
421 in other OCPs ([Barber et al., 2005](#)). HCB has also been measured in the same region in breast
422 milk ([Hassine et al., 2012](#)). Higher concentrations of *p,p'*-DDT compared to their metabolite
423 *p,p'*-DDE are known to indicate recent DDT input ([Iwata et al., 1995](#)). This is the case in
424 Bizerte with *p,p'*-DDT/*p,p'*-DDE ratios > 1 (mean: 3.2). This is consistent with the fact that

425 large amounts of DDT have been recently detected in Menzel Bourguiba city located 24 km
426 SW the sampling site. Hence, some DDT measured in Bizerte aerosols would be likely
427 derived from different regional sources *via* long-range transport. According to wind directions
428 and backward trajectories (Fig. 2), a transportation of DDT from Menzel Bourguiba may
429 occur in winter. In Tunisia, works conducted in 1997 revealed the existence of a number of
430 obsolete stocks of pesticides, containing mostly HCH, DDT (45 tons) and other
431 organochlorines. These pesticides are currently stored in unsatisfactory conditions and can
432 easily disperse into the atmosphere. The ratio of *o,p'*-DDT/*p,p'*-DDT can be used to
433 distinguish technical DDT (low ratio) from “dicofol-type DDT” (high ratio) (Gong et al.,
434 2010). In our case, the *o,p'*-DDT was not detected in any samples, indicating that technical
435 DDT was the main DDT source in the Bizerte aerosols. Similar results were observed by
436 Barhoumi et al. (2014b) in the Bizerte lagoon sediments. Hepchl is the second most abundant
437 compound in our samples, accounting for 10.4% of $\sum_6\text{OCPs}$. Their detection may be related
438 to their use against termites, ants and soil insects, in seed grains and on crops, and in houses
439 (Wang et al., 2008).

440

441 **3.4. Dry deposition and cancer risk assessment**

442

443 The estimation of dry deposition fluxes is relevant to assess the budget of pollutants in the
444 environment and their human health effects (Valotto et al., 2017; Vardar et al., 2002).
445 Detailed information on the dry deposition flux calculation (F , $\text{ng m}^{-2} \text{d}^{-1}$) can be found in the
446 SI (Text S2).

447 For the study period, the average dry deposition fluxes varied from 83.4 to 3070 $\text{ng m}^{-2} \text{d}^{-1}$
448 and from 1157 to 21850 $\text{ng m}^{-2} \text{d}^{-1}$ for $\sum_{34}\text{PAHs}$ and $\sum_{28}\text{AHs}$, respectively. For $\sum_{20}\text{PCBs}$ and
449 $\sum_6\text{OCPs}$ they varied from 60.6 to 1895 $\text{pg m}^{-2} \text{d}^{-1}$ and from 38.2 to 620 $\text{pg m}^{-2} \text{d}^{-1}$, respectively

450 (Table S8). Average daily fluxes were in the range of those reported in other sites (Table S9).
451 The total integrated dry deposition flux ($\sum_{34}\text{PAH}+\sum_{28}\text{AH}+\sum_{20}\text{PCB}+\sum_{6}\text{OCP}$) in the Bizerte
452 area varied from 158 to 22 078 $\text{ng m}^{-2} \text{day}^{-1}$ (Fig. S8). Considering the surface of the Bizerte
453 lagoon as $1.28 \times 10^8 \text{ m}^2$ (Barhoumi et al., 2016), approximately 250 kg yr^{-1} of these chemicals
454 can be deposited to surface waters through aerosols.

455 In this study, inhalation of contaminated aerosols was considered for health risk
456 assessment of PAHs and PCBs. Benzo[a]pyrene (BaP) has been regarded by the World Health
457 Organization (WHO) as the most appropriate indicator to evaluate the carcinogenicity of
458 PAHs in air. Equations used to calculate the total daily carcinogenic potential ($\sum\text{BaP}_{\text{TEQ}}$) of
459 the PAH mixture and lifetime excess cancer risk (ECR) are described in detail in the SI (Text
460 S2).

461 Fig. 4 shows the annual evolution of $\sum\text{BaP}_{\text{TEQ}}$ and ECR for $\Sigma_8\text{PAHs}$. The mean $\sum\text{BaP}_{\text{TEQ}}$
462 for the whole period was 0.19 ng m^{-3} and was 10 times higher in winter (mean: 0.70 ng m^{-3} ;
463 maximal value of 1.49 ng m^{-3} in December) than in summer (mean: 0.07 ng m^{-3} ; minimal
464 value of 0.05 ng m^{-3} in July), indicating a higher health risk during the cold season. BaP was
465 the highest carcinogenic contributor with 37% of the $\sum\text{BaP}_{\text{TEQ}}$, followed by DahA (21%) and
466 BbF (17%). Table S10 shows a comparison of the derived $\sum\text{BaP}_{\text{TEQ}}$ values with those
467 observed in other regions. The $\sum\text{BaP}_{\text{TEQ}}$ values in Bizerte were similar to those in Elche and
468 Zaragoza, Spain (Chofre et al., 2016; Mastral et al., 2003), and lower than those in Algiers
469 (Yassaa et al., 2001), and Venice, Italy (Gregoris et al., 2014). The ECR for a lifetime of 70
470 years ranged from 9×10^{-9} to 1.6×10^{-6} with a mean of 2.1×10^{-7} (Fig. 4), indicating that the
471 lifetime cancer risk from exposure to BaP is negligible in Bizerte ($\text{ECR} < 10^{-6}$), except in
472 winter ($\text{ECR} > 10^{-6}$). These ECR values are much lower than those observed in Beijing and
473 South China (Bandowe et al., 2014).

474

475 **4. Conclusions**

476 For the first time hydrocarbons and organochlorines have been simultaneously measured in
477 aerosol samples from a North African coastal city during one year. Overall, the generated data
478 set is relevant to understand the contribution of the atmospheric pathway to the pollution
479 budget in Bizerte city and very valuable for future evaluations in an area for which little
480 information is available on the atmospheric occurrence and risks of the target contaminants.
481 Further investigations using finer fractions of atmospheric aerosols (PM_{2.5} and PM₁₀) are
482 needed in North African countries such as Tunisia, which have a significantly increasing
483 number of motor vehicles.

484 **Acknowledgements**

485 This work received the financial support of the Institut de Recherche pour le Développement
486 (IRD), through the International Joint Laboratory (LMI) “COSYS-Med”, the Tunisian
487 Ministry of Higher Education and Scientific Research, the PACA region “Particule” project,
488 the IRD-MIO Action Sud “AEROBIZ” project, and the Labex OT-Med (no. ANR-11-LABX-
489 0061) – MEDPOP, funded by the French Government “Investissements d’Avenir” (ANR)
490 through the A*MIDEX project (no ANR-11-IDEX-0001-02). This study is also a contribution
491 to MERMEX/MISTRALS program. We thank the MIO core parameter analytical platform
492 (PAPB) for performing OC and ON analyses. Four anonymous reviewers and associate editor
493 are greatly acknowledged for their constructive comments on the manuscript.

494

495 **Appendix A. Supplementary data**

496 Supplementary data associated with this article can be found in the online version.

497

498

499 **REFERENCES**

- 500 Alves, C., Vicente, A., Pio, C., Kiss, G., Hoffer, A., Decesari, S., Prevôt, A.S.H., Minguillón,
501 M.C., Querol, X., Hillamo, R., Spindler, G., Swietlicki, E., 2012. Organic compounds in
502 aerosols from selected European sites—biogenic versus anthropogenic sources. *Atmos.*
503 *Environ.* 59, 243–255.
- 504 Andreou, G., Alexiou, S.D., Loupa, G., Rapsomanikis, S., 2008. Identification, Abundance
505 and Origin of Aliphatic Hydrocarbons in the Fine Atmospheric Particulate Matter of
506 Athens, Greece. *Water Air Soil Pollut.* 8, 99–106.
- 507 APEK, 2005. Tunisia country situation report. Association for environmental protection in
508 Kerkennah, Tunisia. <http://www.ipen.org>.
- 509 Azimi, S., Rocher, V., Muller, M., Moilleron, R., Thevenot, D.R., 2005. Sources, distribution
510 and variability of hydrocarbons and metals in atmospheric deposition in an urban area
511 (Paris, France). *Sci. Total Environ.* 337, 223–239.
- 512 Bandowe, B.A.M., Meusel, H., Huang, R., Ho, K., Cao, J., Hoffmann, T., Wilcke, W., 2014.
513 PM_{2.5}-bound oxygenated PAHs, nitro-PAHs and parent-PAHs from the atmosphere of a
514 Chinese megacity: Seasonal variation, sources and cancer risk assessment. *Sci. Total.*
515 *Environ.* 473–474, 77–87.
- 516 Barber, J.L., Sweetman, A., Jones, K., 2005. Hexachlorobenzene—sources, environmental fate
517 and risk characterisation. *Euro Chlor.* [http://www.eurochlor.org/media/14951/8-5-9_sd](http://www.eurochlor.org/media/14951/8-5-9_sd_hcb.pdf)
518 [hcb.pdf](http://www.eurochlor.org/media/14951/8-5-9_sd_hcb.pdf).
- 519 Barhoumi, B., El Megdiche, Y., Clérandeau, C., Ben Ameer, W., Mekni, S., Bouabdallah, S.,
520 Derouiche, A., Touil, S., Cachot, J., Driss, M.R., 2016. Occurrence of polycyclic
521 aromatic hydrocarbons (PAHs) in mussel (*Mytilus galloprovincialis*) and eel (*Anguilla*
522 *anguilla*) from Bizerte lagoon, Tunisia, and associated human health risk assessment.
523 *Cont. Shelf Res.* 124, 104–116.

524 Barhoumi, B., Le Menach, K., Devier, M.H., Ameer, W.B., Etcheber, H., Budzinski, H.,
525 Cachot, J., Driss, M.R., 2014b. Polycyclic aromatic hydrocarbons (PAHs) in surface
526 sediments from the Bizerte lagoon, Tunisia: levels, sources and toxicological
527 significance. *Environ. Monit. Assess.* 186, 2653–2669.

528 Barhoumi, B., Le Menach, K., Devier, M.H., El Megdiche, Y., Hammami, B., Ben Ameer,
529 W., Ben Hassine, S., Cachot, J., Budzinski, H., Driss, M.R., 2014a. Distribution and
530 ecological risk of polychlorinated biphenyls (PCBs) and organochlorine pesticides
531 (OCPs) in surface sediments from the Bizerte lagoon, Tunisia. *Environ. Sci. Pollut. Res.*
532 21, 6290–6302.

533 Ben Hassine, S., Hammami, B., Ben Ameer, W., El Megdiche, Y., Barhoumi, B., Driss, M.R.,
534 2014. Particulate Polycyclic Aromatic Hydrocarbons (PAH) in the Atmosphere of
535 Bizerte City, Tunisia. *Bull. Environ. Contam. Toxicol.* 93, 375–382.

536 Berrojalbiz, N., Castro-Jiménez, J., Mariani, G., Wollgast, J., Hanke, G., Dachs, J., 2014.
537 Atmospheric occurrence, transport and deposition of polychlorinated biphenyls and
538 hexachlorobenzene in the Mediterranean and Black seas. *Atmos. Chem. Phys.* 14,
539 8947–8959.

540 Breivik, K., Sweetman, A., Pacyna, J.M., Jones, K.C., 2002. Towards a global historical
541 emission inventory for selected PCB congeners: a mass balance approach 1. Global
542 production and consumption. *Sci. Total Environ.* 290, 181–198.

543 Castro-Jiménez, J., Barhoumi, B., Paluselli, A., Tedetti, M., Jiménez, B., Muñoz-Arnanz, J.,
544 Wortham, H., Driss, M.R., Sempéré, R., 2017. Occurrence, loading and exposure of
545 atmospheric particle-bound POPs at the African and European edges of the western
546 Mediterranean Sea. *Environ. Sci. Technol.* 51, 13180–13189.

547 Castro-Jiménez, J., Berrojalbiz, N., Wollgast, J., Dachs, J., 2012. Polycyclic aromatic
548 hydrocarbons (PAHs) in the Mediterranean Sea: Atmospheric occurrence, deposition
549 and decoupling with settling fluxes in the water column. *Environ. Pollut.* 166, 40–47.

550 Castro-Jiménez, J., Casal, P., González Gaya, B., Pizarro, M., Dachs, J., 2016.
551 Organophosphate ester flame retardants and plasticizers in the global oceanic
552 atmosphere. *Environ. Sci. Technol.* 50, 12831–12839.

553 Castro-Jimenez, J., Dueri, S., Eisenreich, S.J., Mariani, G., Skejo, H., Umlauf, G., Zaldivar,
554 J.M., 2009. Polychlorinated biphenyls (PCBs) in the atmosphere of sub-alpine northern
555 Italy. *Environ. Pollut.* 157, 1024–1032.

556 Castro-Jiménez, J., Mariani, G., Vives, I., Skejo, H., Umlauf, G., Zaldivar, J.M., Dueri, S.,
557 Messiaen, G., Laugier, T., 2011. Atmospheric concentrations, occurrence and
558 deposition of persistent organic pollutants (POPs) in a Mediterranean coastal site (Etang
559 de Thau, France). *Environ. Pollut.* 159, 1948–1956.

560 Chofre, C., Gil-Moltó, J., Galindo, N., Varea, M., Caballero, S., 2016. Characterization of
561 hydrocarbons in aerosols at a Mediterranean city with a high density of palm groves.
562 *Environ. Monit. Assess.* 188, 509–519.

563 Choi, N.R., Lee, S.P., Lee, J.Y., Jung, C.H., Kim, Y.P., 2016. Speciation and source
564 identification of organic compounds in PM₁₀ over Seoul, South Korea. *Chemosphere*
565 144, 1589–1596.

566 Chrysikou, L.P., Samara, C.A., 2009. Seasonal variation of the size distribution of urban
567 particulate matter and associated organic pollutants in the ambient air. *Atmos. Environ.*
568 43, 4557–4569.

569 Cincinelli, A., Mandorlo, S., Dickhut, R.M., Lepri, L., 2003. Particulate organic compounds
570 in the atmosphere surrounding an industrialised area of Prato (Italy). *Atmos. Environ.*
571 37, 3125–3133.

572 Diesch, J.M., Drewnick, F., Zorn, S.R., Von der Weiden-Reinmuller, S.L., Martinez, M.,
573 Borrmann, S., 2012. Variability of aerosol, gaseous pollutants and meteorological
574 characteristics associated with changes in air mass origin at the SW Atlantic coast of
575 Iberia. *Atmos. Chem. Phys.* 12, 3761–3782.

576 Dockery, D.W., Pope III, C.A., Xu, M.D., Spengler, J.D., Ware, J.H., Fay, M.E., Ferris, B.G.,
577 Speizer, F.E., 1993. An association between air pollution and WHO (World Health
578 Organization), 2000. Air Quality Guidelines for Europe. WHO Regional Publications,
579 European Series No. 91, 2nd, (Ed.), WHO, (Eds.), Copenhagen.

580 Draxler, R.R., Rolph, G.D., 2011. HYSPLIT (HYbrid Single- Particle Lagrangian Integrated
581 Trajectory) Model access via NOAA ARL READY. NOAA Air Resources Laboratory:
582 Silver Spring, MD. <http://ready.arl.noaa.gov/HYSPLIT.php>.

583 Dyke, P.H., Foan, C., Fiedler, H., 2003. PCB and PAH releases from power stations and
584 waste incineration processes in the UK. *Chemosphere* 50, 469–480.

585 Gioia, R., Li, J., Schuster, J., Zhang, Y., Zhang, G., Li, X., Spiro, B., Bhatia, R.S., Dachs, J.,
586 Jones, K.C. 2012. Factors affecting the occurrence and transport of atmospheric
587 organochlorines in the China Sea and the northern Indian and South East Atlantic
588 Oceans. *Environ. Sci. Technol.* 46, 10012–10021.

589 Gogou, A., Stephanou, E.G., Stratigakis, N., Grimalt, J.O., Simo, R., Aceves, M., Albaiges, J.,
590 1994. Differences in lipid and organic salt constituents of aerosols from Eastern and
591 Western Mediterranean coastal cities. *Atmos. Environ.* 28, 1301–1310.

592 Gong, P., Wang, X., Sheng, J., Yao, T., 2010. Variations of organochlorine pesticides and
593 polychlorinated biphenyls in atmosphere of the Tibetan Plateau: Role of the monsoon
594 system. *Atmos. Environ.* 44, 2518–2523.

595 Gong, P., Wang, X., Yao, T., 2011. Ambient distribution of particulate- and gas-phase *n*-
596 alkanes and polycyclic aromatic hydrocarbons in the Tibetan Plateau, Environ. Earth
597 Sci. 64, 1703–1711.

598 Górká, M., Rybicki, M., Simoneit, B.R.T., Marynowski, L., 2014. Determination of multiple
599 organic matter sources in aerosol PM₁₀ from Wrocław, Poland using molecular and
600 stable carbon isotope compositions. Atmos. Environ. 89, 739–748.

601 Gregoris, E., Argiriadis, E., Vecchiato, M., Zambon, S., De Pieri, S., Donateo, A., Contini,
602 D., Piazza, R., Barbante, C., Gambaro, G., 2014. Gas-particle distributions, sources and
603 health effects of polycyclic aromatic hydrocarbons (PAHs), polychlorinated biphenyls
604 (PCBs) and polychlorinated naphthalenes (PCNs) in Venice aerosols. Sci. Total.
605 Environ. 476–477, 393–405.

606 Guo, Z.G., Sheng, L.F., Feng, J.L., Fang, M., 2003. Seasonal variation of solvent extractable
607 organic compounds in the aerosols in Qingdao, China. Atmos. Environ. 37, 1825–1834.

608 Haddaoui, I., Mahjoub, O., Mahjoub, B., Boujelben, A., Di Bella, G., 2016. Occurrence and
609 distribution of PAHs, PCBs, and chlorinated pesticides in Tunisian soil irrigated with
610 treated wastewater. Chemosphere 146, 195–205.

611 Hassine, S.B., Ameer, W.B., Gandoura, N., Driss, M.R., 2012. Determination of chlorinated
612 pesticides, polychlorinated biphenyls, and polybrominated diphenyl ethers in human
613 milk from Bizerte (Tunisia) in 2010. Chemosphere 89, 369–377.

614 He, J., Zielinska, B., Balasubramanian, R., 2010. Composition of semi-volatile organic
615 compounds in the urban atmosphere of Singapore: influence of biomass burning.
616 Atmos. Chem. Phys. 10, 11401–11413.

617 Hong, H., Yin, H., Wang, X., Ye, C., 2007. Seasonal variation of PM₁₀-bound PAHs in the
618 atmosphere of Xiamen, China. Atmos. Res. 85, 429–441.

619 Iwata, H., Tanabe, S., Ueda, K., Tatsukawa, R., 1995. Persistent organochlorine residues in
620 air, water, sediments, and soils from the Lake Baikal region, Russia. *Environ. Sci.*
621 *Technol.* 29, 792–801.

622 Karanasiou, A.A., Sitaras, I.E., Siskos, P.A., Eleftheriadis, K., 2007. Size distribution and
623 sources of trace metals and n-alkanes in the Athens urban aerosol during summer.
624 *Atmos. Environ.* 41, 2368–2381.

625 Kim, K.H., Jahan, S.A., Kabir, E., Brown, R.J.C., 2013. A review of airborne polycyclic
626 aromatic hydrocarbons (PAHs) and their human health effects. *Environ. Int.* 60, 71–80.

627 Kishida, M., Mio, C., Imamura, K., Kondo, A., Kaga, A., Shrestha, M., Takenaka, N., Maeda,
628 Y., Sapkota, B., Fujimori, K., 2009. Temporal variation of atmospheric polycyclic
629 aromatic hydrocarbon concentrations in PM₁₀ from the Kathmandu Valley and their
630 gas–particle concentrations in winter. *Int. J. Environ. Anal. Chem.* 89, 67–82.

631 Landlová, L., Čupr, P., Franců, J., Klánová, J., Lammel, G., 2014. Composition and effects of
632 inhalable size fractions of atmospheric aerosols in the polluted atmosphere: Part I.
633 PAHs, PCBs and OCPs and the matrix chemical composition. *Environ. Sci. Pollut. Res.*
634 21, 6188–6204.

635 Lehmler, H.J., Harrad, S.J., Huehnerfuss, H., Kania-Korwel, I., Lee, C.M., Lu, Z., Wong,
636 C.S., 2010. Chiral polychlorinated biphenyl transport, metabolism, and distribution: a
637 review. *Environ. Sci. Technol.* 44, 2757–2766.

638 Mai, B.X., Qi, S.H., Zeng, E.Y., Yang, Q.S., Zhang, G., Fu, J.M., Sheng, G.Y., Peng, P.A.,
639 Wang, Z.S., 2003. Distribution of polycyclic aromatic hydrocarbons in the coastal
640 region off Macao, China: assessment of input sources and transport pathways using
641 compositional analysis. *Environ. Sci. Technol.* 37, 4855–4863.

642 Maioli, O.L.G., Knoppers, B.A., Azevedo, D.A., 2009. Sources, distribution and variability of
643 hydrocarbons in total atmospheric suspended particulates of two Brazilian areas
644 influenced by sugarcane burning. *J. Atmos. Chem.* 64, 159–178.

645 Mandalakis, M., Apostolaki, M., Stephanou, E.G., 2005. Mass budget and dynamics of
646 polychlorinated biphenyls in the eastern Mediterranean Sea. *Global Biogeochem.*
647 *Cycles* 19, 1–16.

648 Mandalakis, M., Tsapakis, M., Tsoga, A., Stefanou, E.G., 2002. Gas-particle concentrations
649 and distribution of aliphatic hydrocarbons, PAHs, PCBs and PCDD/Fs in the
650 atmosphere of Athens (Greece). *Atmos. Environ.* 36, 4023–4035.

651 Manoli, E., Kouras, A., Samara, C., 2004. Profile analysis of ambient and source emitted
652 particle-bound polycyclic aromatic hydrocarbons from three sites in northern Greece.
653 *Chemosphere* 56 867–878.

654 Masih, J., Masih, A., Kulshrestha, A., Singhvi, R., Taneja, A., 2010. Characteristics of
655 polycyclic aromatic hydrocarbons in indoor and outdoor atmosphere in the North
656 central part of India. *J. Hazard Mater.* 177, 190–198.

657 Masiol, M., Formenton, G., Pasqualetto, A., Pavoni, B., 2013. Seasonal trends and spatial
658 variations of PM₁₀-bounded polycyclic aromatic hydrocarbons in Veneto Region,
659 Northeast Italy. *Atmos. Environ.* 79, 811–821.

660 Mastral, A.M., Lopez, J.M., Callen, M.S., García, T., Murillo, R., Navarro, M.V., 2003.
661 Spatial and temporal PAH concentrations in Zaragoza. Spain, *Sci. Total Environ.* 307,
662 111–124.

663 Mazquiarán, M.A.B., de Pinedo, L.C.O., 2007. Organic composition of atmospheric urban
664 aerosol: Variations and sources of aliphatic and polycyclic aromatic hydrocarbons.
665 *Atmos. Res.* 85, 288–299.

666 Mirante, F., Alves, C., Pio, C., Pindado, O., Perez, R., Revuelta, M.A., Artiñano, B., 2013.
667 Organic composition of size segregated atmospheric particulate matter, during summer
668 and winter sampling campaigns at representative sites in Madrid, Spain. *Atmos. Res.*
669 132–133, 345–361.

670 Moussaoui, Y., Balducci, C., Cecinato, A., Meklati, B.Y., 2013. Atmospheric particulate
671 organic matter at urban and forest sites of Northern Algeria. *Urban Climate* 4, 85–101.

672 Nizzetto, L., Macleod, M., Borgå, K., Cabrerizo, A., Dachs, J., Di Guardo, A., Ghirardello,
673 D., Hansen, K.M., Jarvis, A., Lindroth, A., Ludwig, B., Monteith, D., Perlinger, J.A.,
674 Scheringer, M., Schwendenmann, L., Semple, K.T., Wick, L.Y., Zhang, G., Jones, K.C.,
675 2010. Past, Present, and Future Controls on Levels of Persistent Organic Pollutants in
676 the Global Environment. *Environ. Sci. Technol.* 44, 6526–6531.

677 Ouakad, M., 2007. Genèse et évolution des milieux laguno-lacustres du Nord-Est de la
678 Tunisie (Garaet el Ichkeul, Lagunes de Bizerte et Ghar el Mehl). Ph.D., Faculté des
679 Sciences de Tunis.

680 Ozcan, S., Aydin, M.E., 2009. Polycyclic aromatic hydrocarbons, polychlorinated biphenyls
681 and organochlorine pesticides in urban air of Konya, Turkey. *Atmos. Res.* 93, 715–722.

682 Park, S.S., Kim, Y.J., Kang, C.H., 2002. Atmospheric polycyclic aromatic hydrocarbons in
683 Seoul, Korea. *Atmos. Environ.* 36, 2917–2924.

684 Pegoraro, C.N., Harner, T., Su, K., Chiappero, M.S., 2016. Assessing levels of POPs in air
685 over the South Atlantic Ocean off the coast of South America. *Sci. Total. Environ.* 571,
686 172–177.

687 Perrone, M.G., Carbone, C., Faedo, D., Ferrero, L., Maggioni, A., Sangiorgi, G., Bolzacchini,
688 E., 2014. Exhaust emissions of polycyclic aromatic hydrocarbons, *n*-alkanes and
689 phenols from vehicles coming within different European classes. *Atmos. Environ.* 82,
690 391–400.

691 Piazza, R., Gambaro, A., Argiriadis, E., Vecchiato, M., Zambon, S., Cescon, P., Barbante, C.,
692 2013. Development of a method for simultaneous analysis of PCDDs, PCDFs, PCBs,
693 PBDEs, PCNs and PAHs in Antarctic air. *Anal. Bioanal. Chem.* 405, 917–932.

694 Raimbault, P., Garcia, N., Cerrutti, F., 2008. Distribution of inorganic and organic nutrients in
695 the South Pacific Ocean. Evidence for long-term accumulation of organic matter in
696 nitrogen-depleted waters. *Biogeosciences* 5, 281–298.

697 Ramírez, N., Cuadras, A., Rovira, E., Marcé, R.M., Borrull, F., 2011. Risk assessment related
698 to atmo-spheric polycyclic aromatic hydrocarbons in gas and particle phases near
699 industrial sites. *Environ. Health Perspect.* 119, 1110–1116.

700 Ravindra, K., Sokhi, R., Grieken, R.V., 2008. Atmospheric polycyclic aromatic
701 hydrocarbons: source attribution, emission factors and regulation. *Atmos. Environ.* 42,
702 2895–2921.

703 Rogge, W.F., Hildemann, L.M., Mazurek, M.A., Cass, G.R., Simoneit, B.R.T., 1993b.
704 Sources of fine organic aerosol. 2. Noncatalyst and catalyst-equipped automobiles and
705 heavy duty diesel trucks. *Environ. Sci. Technol.* 27, 636–651.

706 Rogge, W.F., Hildemann, L.M., Mazurek, M.A., Cass, G.R., Simoneit, B.R.T., 1996.
707 Mathematical modeling of atmospheric fine particle-associated primary organic
708 compound concentrations. *J. Geophys. Res.* 101, 19541–19549.

709 Rogge, W.F., Mazurek, M.A., Hildemann, L.M., Cass, G.R., Simoneit, B.R.T., 1993a.
710 Quantification of urban organic aerosols at a molecular level: identification, abundance
711 and seasonal variation. *Atmos. Environ.* 27A, 1309–1330.

712 Scholtz, M.T., Bidleman, T.F., 2006. Modelling of the long term fate of pesticide residues in
713 agricultural soils and their surface exchange with the atmosphere: part I. Model
714 description and evaluation. *Sci. Total Environ.* 368, 823–838.

715 Schröder, C.H.K., Pinhel, M.F.M., Mendonça, A.O., 2016. The Brazilian strategy for
716 monitoring persistent organic pollutants in food obtained from animals. *Sci. Total.*
717 *Environ.* 573, 1370–1379.

718 Stern, G.A., Halsall, C.J., Barrie, L.A., 1997. Polychlorinated biphenyls in Arctic air. 1.
719 Temporal and spatial trends: 1992-1994. *Environ. Sci. Technol.* 31, 3619–3628.

720 Takasuga, T., Senthilkumar, K., Matsumura, T., Shiozaki, K., Sakai, S.I., 2006. Isotope
721 dilution analysis of polychlorinated biphenyls (PCBs) in transformer oil and global
722 commercial PCB formulations by high resolution gas chromatography–high resolution
723 mass spectrometry. *Chemosphere* 62, 469–484.

724 Tang, N., Hattori, T., Taga, R., Igarashi, K., Yang, X.Y., Tamura, K., Kakimoto, H.,
725 Mishukov, V.F., Toriba, A., Kizu, R., 2005. Polycyclic aromatic hydrocarbons and
726 nitropolycyclic aromatic hydrocarbons in urban air particulates and their relationship to
727 emission sources in the Pan–Japan Sea countries. *Atmos. Environ.* 39, 5817–5826.

728 Tobiszewski, M., Namieśnik, J., 2012. PAH diagnostic ratios for the identification of
729 pollution emission sources. *Environ. Pollut.* 162, 110–119.

730 Valotto, G., Rampazzo, G., Gonella, F., Formenton, G., Ficotto, S., Giraldo, G., 2017. Source
731 apportionment of PAHs and n-alkanes bound to PM₁ collected near the Venice
732 highway. *J. Environ. Sci.* 54, 77–89.

733 Vardar, N., Odabasi, M., Holsen, T.M., 2002. Particulate dry deposition and overall
734 deposition velocities of polycyclic aromatic hydrocarbons. *J. Environ. Eng.* 128, 269–
735 274.

736 Wan, X., Chen, J., Tian, F., Sun, W., Yang, F., Saiki, K., 2006. Source apportionment of
737 PAHs in atmospheric particulates of Dalian: factor analysis with nonnegative
738 constraints and emission inventory analysis. *Atmos. Environ.* 40, 6666–6675.

739 Wang, G., Huang, L., Zhao, X., Niu, H., Dai, Z., 2006. Aliphatic and polycyclic aromatic
740 hydrocarbons of atmospheric aerosols in five locations of Nanjing urban area, China.
741 Atmos. Res. 81, 54–66.

742 Wang, X., Li, X., Cheng, H., Xu, X., Zhuang, G., Zhao, C., 2008. Organochlorine pesticides
743 in particulate matter of Beijing, China. J. Hazard. Mater. 155, 350–357.

744 Wania, F., Mackay, D., 1996. Tracking the distribution of persistent organic pollutants.
745 Environ. Sci. Technol. 30, 390A–396A.

746 WHO, 2000. Air Quality Guidelines for Europe. WHO Regional Publications, European
747 Series No. 91, second ed. WHO, Copenhagen.

748 Wolska, L., 2002. Miniaturised analytical procedure of determining polycyclic aromatic
749 hydrocarbons and polychlorinated biphenyls in bottom sediments. J. Chromatogr. A
750 959, 173–180.

751 Wu, Y., Yang, L., Zheng, X., Zhang, S., Song, S., Li, J., Hao, J., 2014. Characterization and
752 source apportionment of particulate PAHs in the road side environment in Beijing. Sci.
753 Total Environ. 470–471, 76–83.

754 Yao, Z.W., Jiang, G.B., Xu, H.Z., 2002. Distribution of organochlorine pesticides in seawater
755 of the Bering and Chukchi Sea. Environ. Pollut. 116, 49–56.

756 Yassaa, N., Youcef Meklati, B., Cecinato, A., Marino, F., 2001. Particulate *n*-alkanes, *n*-
757 alkanolic acids and polycyclic aromatic hydrocarbons in the atmosphere of Algiers City
758 Area. Atmos. Environ. 35, 1843–1851.

759 Yeo, H.G., Choi, M., Chun, M.Y., Kim, T.W., Cho, K.C., Sunwoo, Y., 2004. Concentration
760 characteristics of atmospheric PCBs for urban and rural area, Korea. Sci. Total Environ.
761 324, 261–270.

762 Yeo, H.G., Choi, M., Chun, M.Y., Sunwoo, Y., 2003. Concentration distribution of
763 polychlorinated biphenyls and organochlorine pesticides and their relationship with
764 temperature in rural air of Korea. *Atmos. Environ.* 37, 3831–3839.

765 Yunker, M.B., Macdonald, R.W., Vingarzan, R., Mitchell, R.H., Goyette, D., Sylvestre, S.,
766 2002. PAHs in the Fraser River basin: a critical appraisal of PAH ratios as indicators of
767 PAH source and composition. *Org. Geochem.* 33, 489–515.

768 Zheng, M., Fang, M., Wang, F., To, K.L., 2000. Characterization of the solvent extractable
769 organic compounds in PM_{2.5} aerosols in Hong Kong. *Atmos. Environ.* 34, 2691–2702.

770 Zheng, M., Salmon, L.G., Schauer, J.J., Zeng, L., Kiang, C.S., Zhang, Y., Cass, G.R., 2005.
771 Seasonal trends in PM_{2.5} source contributions in Beijing, China. *Atmos. Environ.* 39,
772 3967–3976.

773

774

775

776

777

778

779

780

781

782

783

784

785

786

787 **Figure captions**

788

789 **Figure 1.** Total PAH (A), AH (B), PCB (C) and OCP (D) concentrations in aerosol samples
790 of Bizerte city from March 2015 to January 2016.

791 **Figure 2.** The dominant wind directions and five day backward trajectories in Bizerte city
792 during the four seasons (for backward trajectories, colors denote different air-mass movement
793 and the figures in the lower frames are altitude in meters).

794 **Figure 3.** Pearson principal component analysis (loading plots (A) and score plots (B)) for
795 TSP, OC, ON, chemical (\sum_{34} PAHs, \sum_{28} AHs, \sum_{20} PCBs, \sum_6 OCPs) and meteorological (AT,
796 WS, RH) variables for aerosol samples of Bizerte city. TSP – total suspended particles, OC –
797 organic carbon, ON – organic nitrogen, WS –wind speed, RH – relative humidity, AT –
798 ambient temperature, AHs – aliphatic hydrocarbons, PAHs – polycyclic aromatic
799 hydrocarbons, PCBs – polychlorinated biphenyls, OCPs – organochlorine pesticides. Green,
800 blue, black and red colors indicate the seasons of spring, summer, autumn and winter,
801 respectively.

802 **Figure 4.** \sum BaP_{TEQ} and excess cancer risk (ECR) in Bizerte city from March 2015 to January
803 2016.

804

805

806

807

808

809

810

811

812 **Table captions**

813

814 **Table 1.** Diagnostic indices and ratios of PAHs and AHs for aerosol samples of Bizerte city at

815 the four seasons.

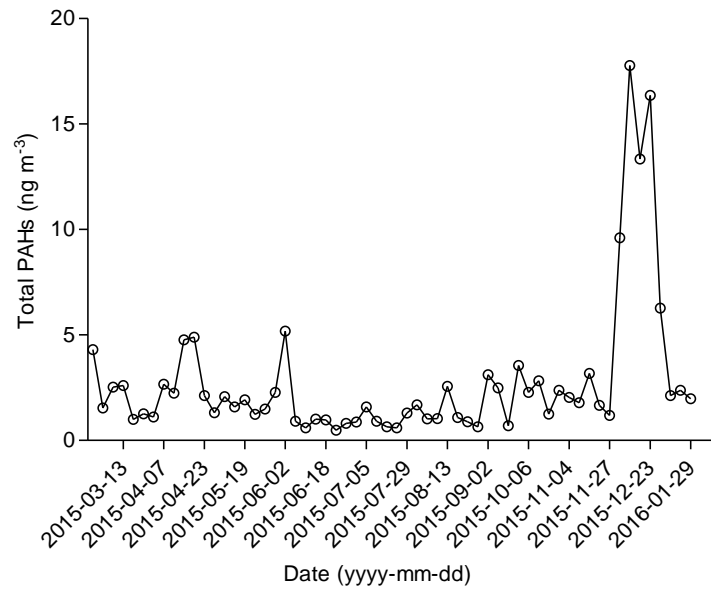
816

817

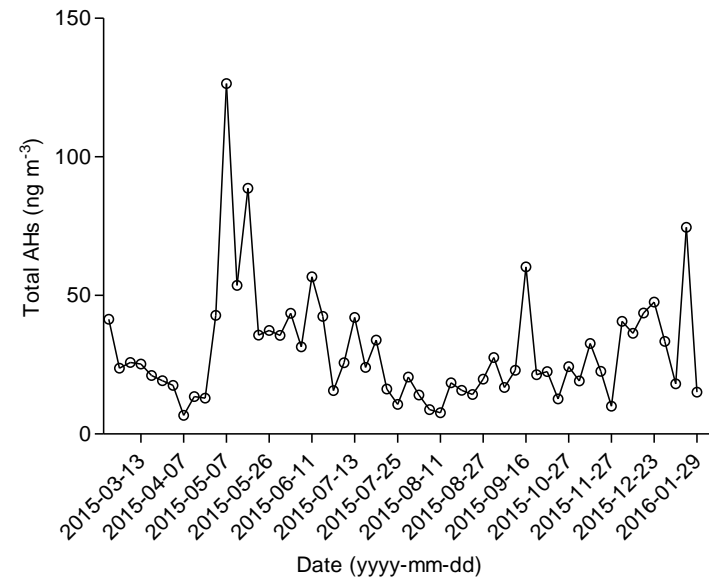
818

Figure 1

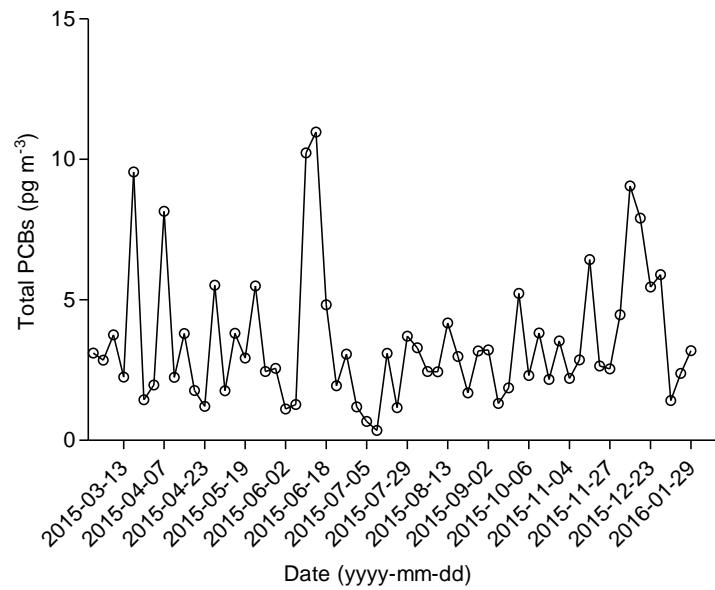
(A)



(B)



(C)



(D)

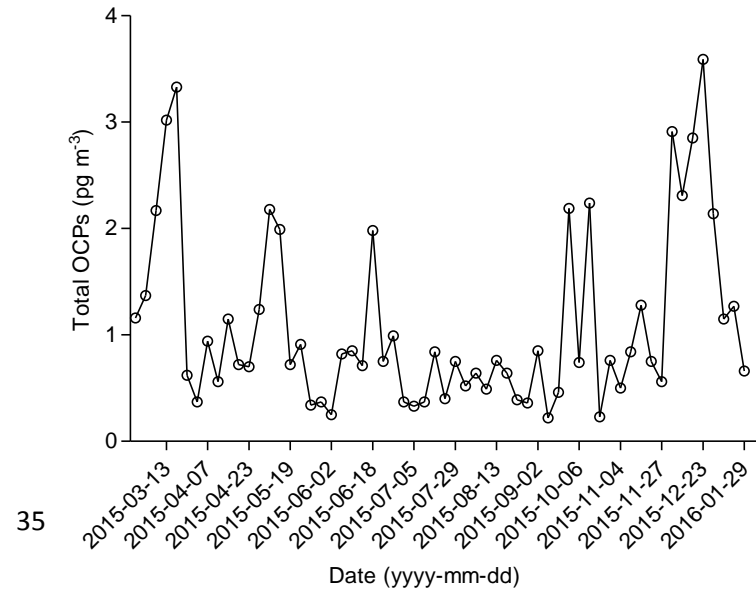
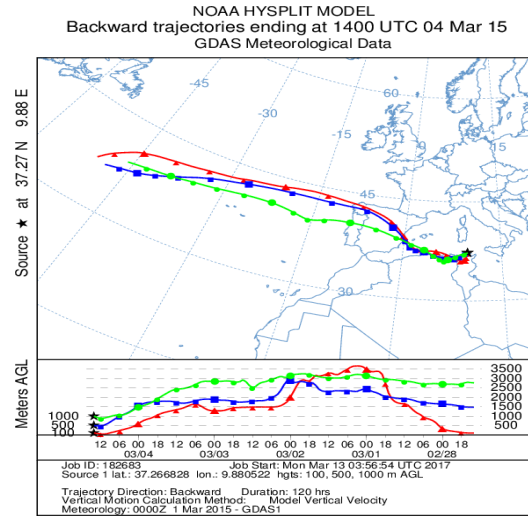
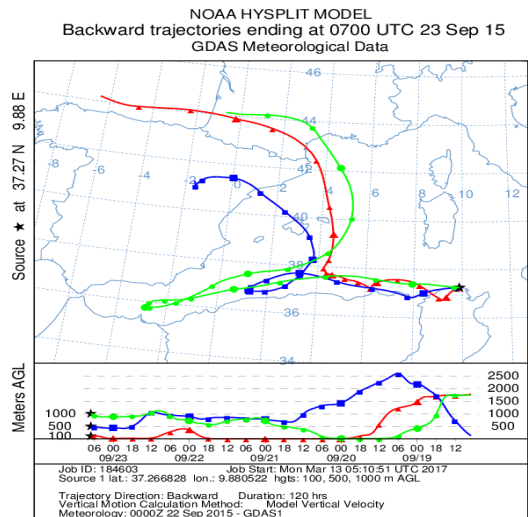


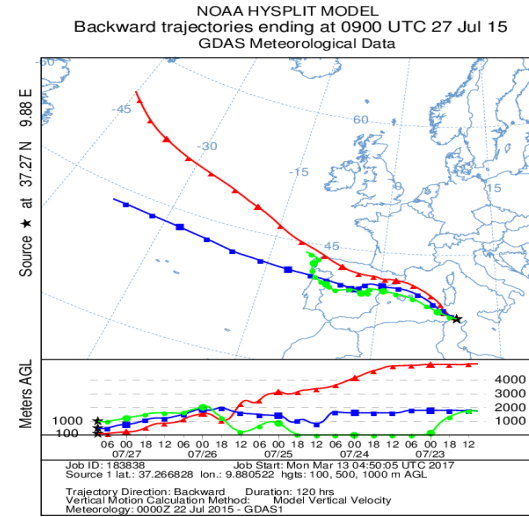
Figure 2



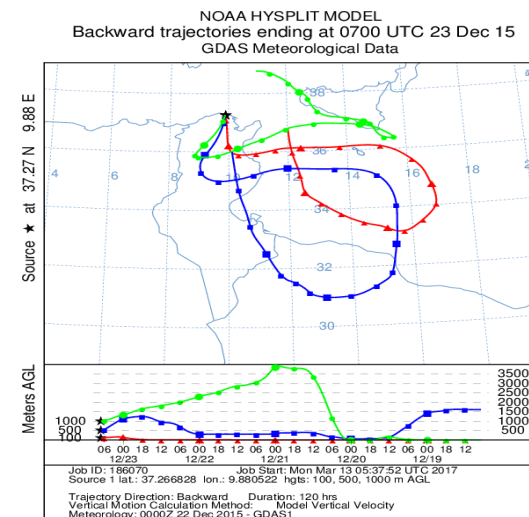
Spring



Autumn



Summer



Winter

Figure 3

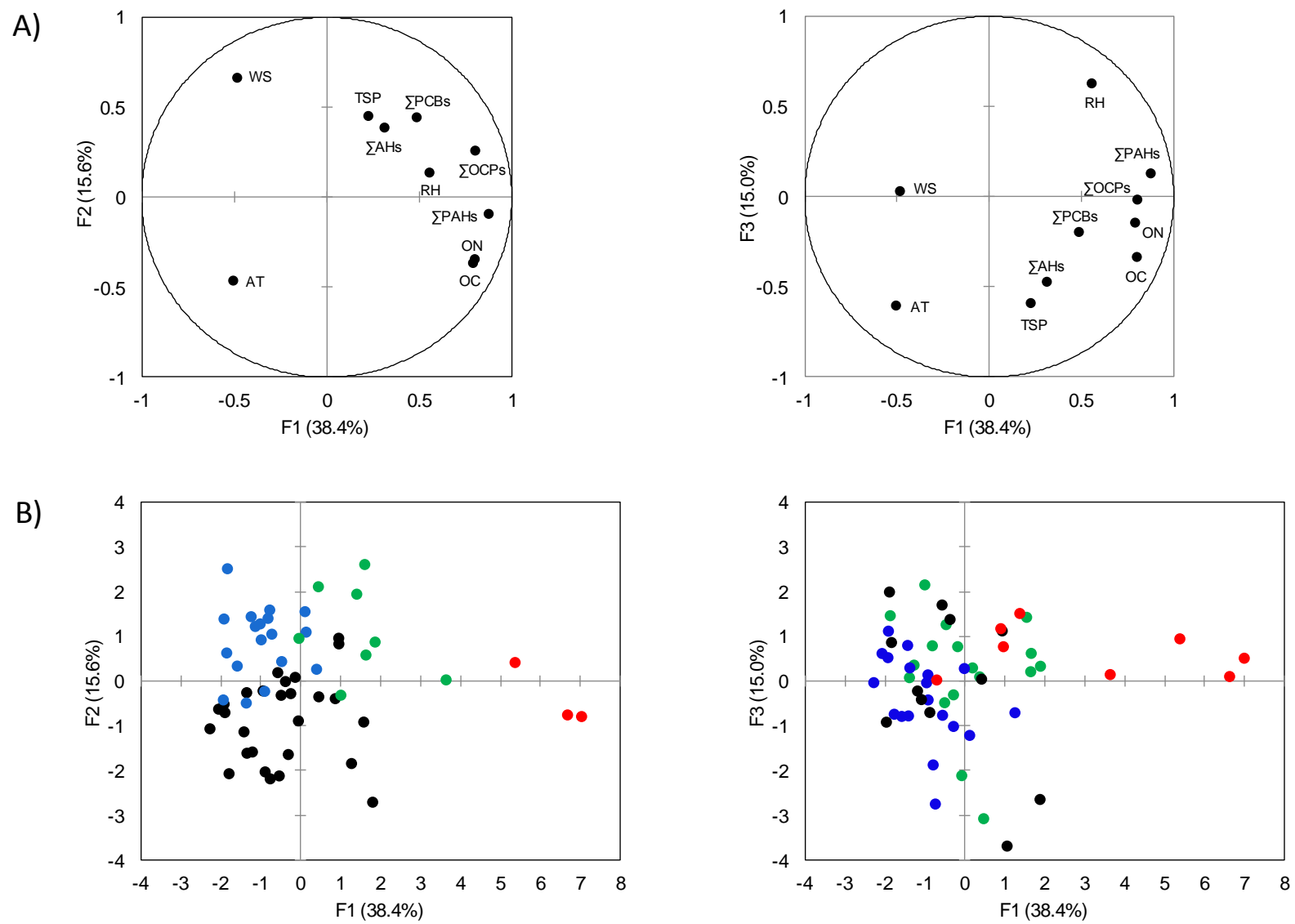


Figure 4

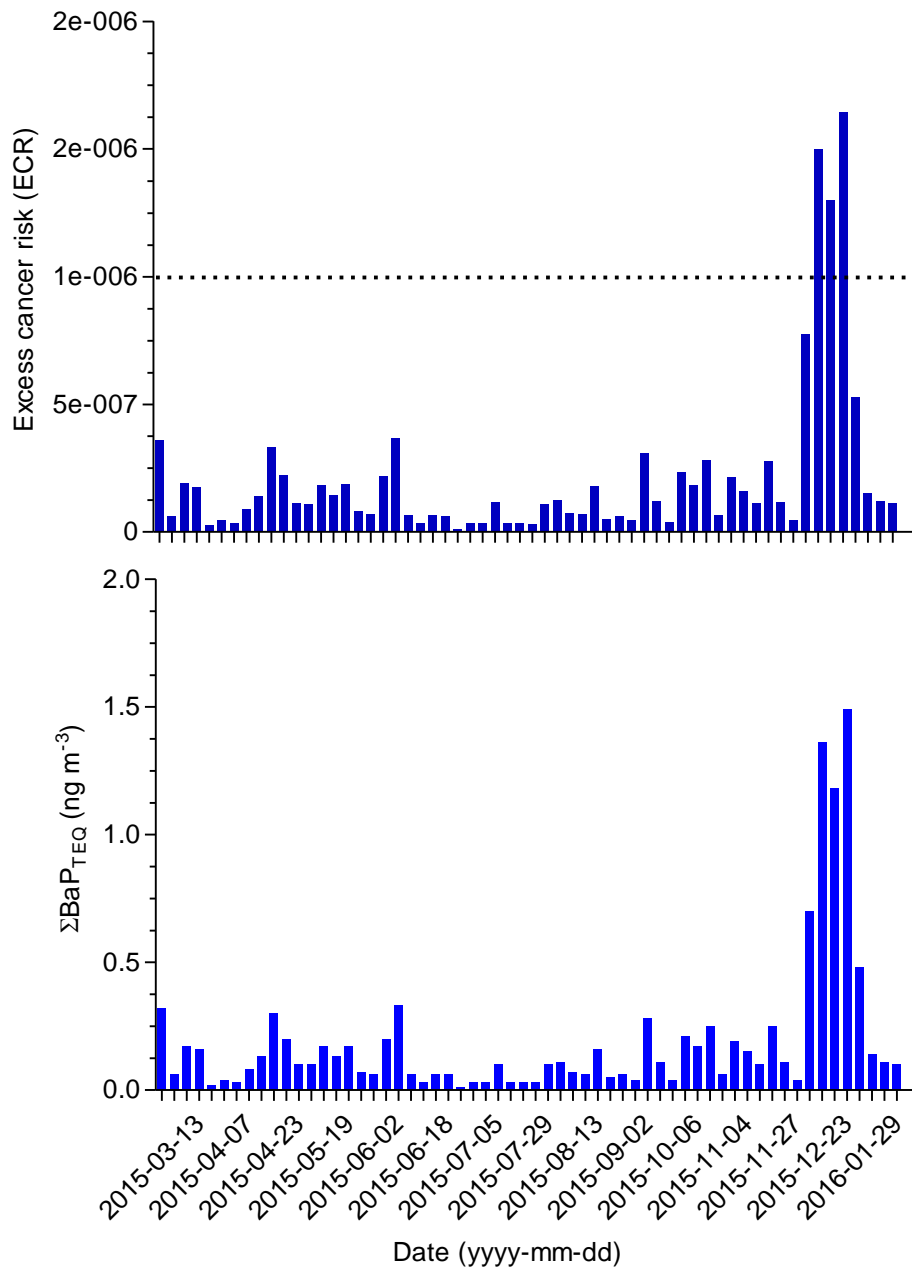


Table 1. Diagnostic indices and ratios of PAHs and AHs for aerosol samples of Bizerte city at the four seasons.

Index or ratio	Spring		Summer		Autumn		Winter		Annual	
	Mean	Range								
PAHs										
Ant/(Ant + Phe)	0.11	0.00–0.31	0.14	0.00–0.25	0.11	0.03–0.18	0.10	0.06–0.12	0.12	0.00–0.31
BaA/(BaA + Chr)	0.18	0.08–0.24	0.24	0.06–0.40	0.27	0.17–0.39	0.24	0.17–0.29	0.23	0.06–0.40
Flu/(Flu + Pyr)	0.47	0.28–0.67	0.41	0.25–0.48	0.44	0.36–0.52	0.46	0.43–0.51	0.44	0.25–0.67
IcdP/(IcdP + BghiP)	0.39	0.28–0.49	0.40	0.23–0.49	0.39	0.31–0.52	0.41	0.36–0.46	0.39	0.23–0.52
BbF/BkF	3.05	2.26–4.25	3.93	1.74–12.4	3.85	3.29–4.75	3.93	3.11–4.63	3.63	1.74–12.4
CPAHs/ \sum_{16} US EPA PAHs ^a	0.91	0.83–0.95	0.89	0.84–0.92	0.91	0.84–0.93	0.94	0.91–0.96	0.91	0.83–0.96
AHs										
CPI ₁ ^b	2.49	1.38–6.12	2.76	1.69–5.91	1.58	1.07–2.38	1.84	1.27–5.04	2.29	1.07–6.12
CPI ₂ ^c	1.57	1.06–2.23	1.72	0.96–8.40	1.71	1.47–1.94	1.44	1.32–1.70	1.63	0.96–8.40
CPI ₃ ^d	3.64	2.11–7.96	3.70	1.91–8.84	1.81	1.21–2.85	2.46	1.62–7.07	3.10	1.21–8.84
%Wax ^e	39.9	19.3–72.8	45.0	27.3–73.0	22.9	5.9–42.0	23.4	13.1–67.9	35.6	5.9–73.0
UCM (ng m ⁻³)	118.0	24.8–262.5	71.7	22.6–109.1	81.6	22.5–169.3	153.9	32.1–254.9	99.6	22.5–262.5
Pr/Phy	0.95	0.00–2.10	1.59	0.00–6.77	1.40	0.00–14.6	0.03	0.00–0.25	1.13	0.00–14.6

^aCPAHs = combustion PAHs = Flu+Pyr+BaA+Chr+BbF+BkF+BaP+IcdP+BghiP.

^bCPI₁ = $\Sigma(n-C_{15}-n-C_{39})/\Sigma(n-C_{16}-n-C_{40})$, CPI for the whole range.

^cCPI₂ = $\Sigma(n-C_{15}-n-C_{25})/\Sigma(n-C_{16}-n-C_{24})$, CPI for petrogenic *n*-alkanes.

^dCPI₃ = $\Sigma(n-C_{25}-n-C_{35})/\Sigma(n-C_{26}-n-C_{36})$, CPI for biogenic *n*-alkanes.

^eWax $C_n = [C_n] - [C_{n+1} + C_{n-1}] \times 0.5$ (1), %Wax = $(\Sigma Wax C_n \times 100)/\Sigma C_n$, negative values of C_n were replaced by zero.